

# AEROSOL CLASSIFICATION IN CYPRUS USING ACTIVE AND PASSIVE REMOTE SENSING TECHNIQUES

Savva A. <sup>\*a,b</sup>, Nisantzi A. <sup>a,b</sup>, Ansmann A. <sup>c</sup>, Hadjimitsis D. <sup>a,b</sup>, Mamouri R.E. <sup>a,b</sup>

<sup>a</sup> Eratosthenes Centre of Excellence, 3012 Limassol, Cyprus; <sup>b</sup> Department of Civil Engineering & Geomatics, Cyprus University of Technology, 3036 Limassol, Cyprus; <sup>c</sup> Leipzig Institute for Tropospheric Research, 04318 Leipzig, Germany

## ABSTRACT

Limassol region in Cyprus, located in the Eastern Mediterranean, represents a major crossroads for various air masses, making the place a hub for mixing particles from both local and remote aerosol sources. The unique atmospheric conditions of the area offer an ideal place to study the vertical atmospheric structure. This study utilizes active and passive remote sensing techniques, such as the sun-photometer AERONET CUT-TEPAK station (Aerosol Robotic Network) and the Polly XT Raman LIDAR depolarization system available in Limassol (34.7°N, 33°E). An extended analysis of long-term ground-based measurements using AERONET Level 2.0 solar products is presented. The study focuses on the classification method proposed by Toledano et al. (2007) [1] for different aerosol types. Aerosol optical depth at 440 nm (AOD) and Ångström Exponent at 440-870 nm (AE) are examined for 14 years (2010 - 2023). The results show a strong contribution of dust particles in spring months and continental particles in summer periods. Marine particles were found to be extremely dominant according to the classification. Subsequently, to examine the presence of dust particles in the marine's classification, the study incorporates the particle depolarization ratio (PDR) from the LIDAR vertical profiles at 532 nm using the Klett method. Thus, a new aerosol scheme has been developed concluding in four aerosol categories (dominating conditions of marine aerosol (M), mineral dust (D), anthropogenic haze/ biomass burning (H+S), mixed aerosol).

**Keywords:** \*Remote Sensing, Aerosol, Aerosol classification, Eastern Mediterranean, Cyprus, marine aerosol\*  
\*athina.savva@eratosthenes.org.cy; phone +357 99395315

## 1. INTRODUCTION

Atmospheric aerosols originating from both natural sources and anthropogenic activities have a significant role in impacting human health, shaping the environment, and influencing climate change patterns [2]. Owing to the diversity of the aerosol sources and their complex optical properties, aerosols continue to be a major uncertainty in the climate system [3]. Depending on the region, different types or mixtures of aerosols can cause a positive or negative effect on radiation forcing [4], [5]. To better understand the impact of aerosols on radiation and climate, it is necessary to study the aerosols' optical and microphysical characteristics and examine the various types in different sites around the globe.

In the present study, the region that is examined is the Eastern Mediterranean, Limassol city in Cyprus. Due to its geographical location, the Eastern Mediterranean receives particles of various kinds due to their diverse areas of origin. Dust particles from the Sahara Desert and Middle Eastern regions, marine aerosols, anthropogenic particles from urban/industrial areas from North Africa, Eastern and Central Europe, and biomass burning particles from neighboring regions (e.g., Turkey) [6], [7], [8], [9], [10] are some of the dominant particles in the atmosphere of Mediterranean region. It is therefore a suitable point for studying the vertical distribution of suspended particles.



Figure 1. MODIS Satellite Image (10/10/2022, <https://worldview.earthdata.nasa.gov>) showing the regions of the Eastern Mediterranean, North Africa, and Middle East.

Classification of different types and mixtures of aerosols has been a major concern of the scientific community and for this reason various classification methods have been proposed in literature. Numerous studies focus on the characterization of aerosols utilizing in-situ measurements, either remote sensing techniques as ground-based, airborne or satellite to retrieve the optical properties of the aerosols [11], [12], [13], [14]. Considering the sparse nature of ground-based optical measurement networks, estimates of the time variation and spatial distribution of aerosols often rely on satellite remote sensing [15], [16], [17]. However, due to the high uncertainty of the satellite products, the calibration and validation of these instruments measurements is performed either from ground-based remote sensing techniques or in-situ measurements. Remote sensing techniques are utilized for retrieving data of optical properties of aerosols [1], [18], [19], [20], [21], [22], [23], [24]. The identification of suspended particle types utilizing remote sensing techniques, mostly studies the relationship between aerosol load and aerosol size. The main aerosol types characterized by remote sensing optical properties retrievals are dust, marine, particles from biomass burning (BB: biomass burning), urban / anthropogenic haze and continental particles [1], [25]. The global AERONET network (Aerosol Robotic Network) is the base of remote sensing techniques for the aerosol characterization studies, worldwide [18], [19], [20], [22], [26], [27]. However the synergic use of remote sensing techniques, in particular depolarization LIDAR and sun-photometer can be effectively conduct the exploration of optical and microphysical properties of diverse aerosol types [9], [10], [28], [29], [30], [31], [32]. Aerosol Optical Depth (AOD) and the Ångström Exponent (AE) are used to define aerosols [1], [25], [26], [35]. AOD is the amount of aerosols in the vertical column of the atmosphere and the Ångström Exponent is an index that indicates the size of particles [33] and classifies them into fine and coarse mode [34], [35]. In the literature the most common categorization of aerosol using these properties is into dust, marine particles/sea salt, urban/industrial/continental particles produced by fossil fuel combustion, particles from biomass burning/coal combustion/fire smoke and mixed aerosols [20], [26], [36]. Aerosols can be classified based on their shape (spherical, non-spherical), by particle depolarization ratio at various wavelengths with depolarization and Raman LIDAR. Depolarization ratio is a valuable property for studying aerosols and clouds [37], as it effectively distinguishes spherical particles from non-spherical particles, providing insights into mixed-phase clouds by discriminating water layers from ice layers [38]. Distinct values of particle depolarization ratio [PDR] have been delved into by numerous studies. Relevant examples of PDR at 355, 532 nm for desert dust are for Sahara and Middle East  $25 \pm 3$ ,  $30 \pm 1$  respectively. For biomass burning / smoke at 532 nm,  $5 \pm 1$  [28]. Marine aerosols have minimum values of PDR at 355, 532 nm,  $2 \pm 2$  and  $2 \pm 1$  respectively [39], [40] and the values of PDR of volcanic ash is between 0.30 - 0.35 [41].

## 2. DATA & METHODOLOGY

### 2.1 Instrumentation

This study was conducted using data from Cimel sun-photometer of AERONET (Aerosol Robotic Network) that has been operated at Limassol (CUT-TEPAK station) since 2010 [42], [43]. The instrument allows measurements of direct and diffuse solar radiation directly from the sun and sky respectively, at wavelengths 340, 380, 440, 500, 670, 870, 1020 and 1640 nm [4]. Microphysical and optical properties of the aerosols can be retrieved from the sun-photometer, thus in this study the products that used are Aerosol Optical Depth (AOD) and Ångström Exponent 440-870 nm ( $\alpha$  ή AE). Also, at the Cyprus Atmospheric Remote Sensing Observatory (CARO) of the Eratosthenes Centre of Excellence at Limassol (34.7°N, 33°E, 2.8 m a.s.l.), a multiwavelength polarization Raman lidar, Polly (PORTabLe Lidar sYstem) [45], utilized to monitor aerosol layers and clouds. CARO is part of the ACTRIS (Aerosols, Clouds and Trace gases Research InfraStructure) National Facility of the Republic of Cyprus for the remote sensing of aerosols and clouds [46]. The retrievals of the polarization Raman Lidar are the vertical profiles of backscatter coefficient ( $\beta$ ) of the particles at 355, 532 and 1064 nm, the particle extinction coefficient ( $a$ ) at 355 and 532 nm, the lidar ratios ( $S$ ) as well as the volume (VDR) and particle linear depolarization ratio (PLDR) at 355 and 532 nm. In this study, the vertical distributions of the particle depolarization ratio at 532 nm by the Klett method [47] were used.

### 2.2 Aerosol classification for Limassol area

An aerosol classification method proposed by Toledano et al. (2007) [1] is performed for the Limassol area. The categorization is carried out by delimitation of optical properties of aerosols, the aerosol optical depth (AOD) at 440 nm and the Ångström Exponent (AE) at 440-870 nm. The aerosol classification is performed at CUT-TEPAK site in Limassol for the period 2010-2023 (14 years), using the level 2.0 products of the Cimel, sun-photometer of the AERONET network. According to this classification, particulate matter is divided into five (5) categories, desert dust, marine, continental, biomass burning particles and mixed aerosols (desert dust and biomass burning). The thresholds for each category are presented in Table 1.

Table 1. Aerosol classification thresholds by Toledano et al. (2007) [1].

Aerosol type	AOD (440 nm)	AE (440-870 nm)
Desert dust	-	$\leq 1.05$
Marine	$\leq 0.2$	0-2
Continental	0.2 - 0.35	$\geq 1.05$
Biomass burning	$\geq 0.35$	$\geq 1.4$
Mixed aerosol	$\geq 0.35$	1.05 - 1.4

### 2.3 Study of marine aerosol classification area with Particle Depolarization ratio

According to the classification method proposed by Toledano et al. (2007) [1], marine particles were found to be extremely dominant in the coastal city of Limassol. Marine aerosol often is a mixture of anthropogenic haze, continental and marine particles posing challenges to explain the pure marine aerosol. The characterization of marine aerosol for the Mediterranean Sea becomes crucial because of the influence of nearby areas and the restricted basin dimension [48]. Subsequently, a study utilizing the particle depolarization ratio (PDR) was performed in the marine area of the aerosol classification according to Toledano's et al. (2007) method [1]. This approach was used to investigate the presence of dust in the marine particles area categorizing particles into spherical and non-spherical. The information is derived from the LIDAR vertical profiles at 532 nm using the Klett method, conducted in the range of  $AOD \leq 0.2$  and  $AE \leq 1$  (marine area) for the period 2016-2018 & 2020-2023 (available LIDAR data). In this study the criteria for pure marine by Smirnov et

al. (2003) [49]  $AOD < 0.2$  and  $AE \leq 1$  are used, including also the 0.2 values of AOD. Particle depolarization values are the average value of the depolarization ratio of the aerosol layer for the date and time of each measurement, calculated. The vertical profiles of PDR of the aerosol layers were retrieved from the PollyNET LIDAR page (<https://polly.tropos.de/>) for Limassol LIDAR site which is operated at CARO station, of Eratosthenes Centre of Excellence. For the characterization of aerosols, the thresholds of particle depolarization ratio at 532 nm for six aerosol types from a study conducted for the Limassol region by (PhD Argyro Nisantzi, 2015) [50] were used.

Table 2. Particle depolarization ratio per aerosol type at 532 nm, thresholds for Limassol region (PhD Argyro Nisantzi, 2015).

<b>Aerosol type</b>	<b>Particle depolarization ratio (PDR – <math>\delta</math> at 532 nm)</b>
Biomass burning	$0.121 \pm 0.021$
Urban haze	$0.067 \pm 0.032$
Continental particles	$0.083 \pm 0.021$
Marine particles	$0.032 \pm 0.021$
Saharan dust	$0.239 \pm 0.07$
Middle east dust	$0.237 \pm 0.049$

#### 2.4 Aerosol classification based on Limassol atmospheric (aerosol optical properties) observations.

A new aerosol typing scheme based on spectrally resolved long-term LIDAR and sun-photometer observations at Limassol has been implemented. The scheme draws on clean marine aerosol conditions observations and on two decades of AERONET-based observations of heavy dust pollution around the world. An analysis to characterize the dominant aerosols observed in Limassol atmosphere is conducted. Clear sectors are defined based on observed patterns to understand the local atmospheric dynamics. The aerosols are categorized into dominating marine aerosol conditions (M), dominating mineral dust conditions (D), dominating anthropogenic haze / biomass burning conditions (H+S) and mixed aerosol. The categorization is carried out by delimitation of optical properties of aerosols, the aerosol optical depth (AOD) at 440 nm and the Ångström Exponent (AE) at 440-870 nm. The aerosol classification is performed at CUT-TEPAK station in Limassol site for the period 2016-2018 & 2020-2023 (available Lidar data), using the level 2.0 products of the Cimel, sun-photometer of the AERONET network. The thresholds of each category are presented in Table 3.

Table 3. Aerosol classification thresholds based on observations of aerosol properties at Limassol.

<b>Aerosol type</b>	<b>AOD (440 nm)</b>	<b>AE (440-870 nm)</b>
Dominating marine aerosol conditions	$< 0.08$	$< 0.75$
Dominating mineral dust conditions	$> 0.12$	$< 0.6$
Dominating anthropogenic haze / biomass burning conditions	$> 0$	$> 1.2$
Mixed aerosol	All the other parts	All the other parts

### 3. RESULTS & DISCUSSION

#### 3.1 Aerosol classification method proposed in literature.

This aerosol characterization method is based on two microphysical aerosol optical properties: the Aerosol Optical Depth (AOD) and the Ångström Exponent (AE). Therefore, the AOD 440 nm vs AE 440-870 nm diagram qualitatively illustrates the quantity and size of particles observed in atmosphere (Figure 2).

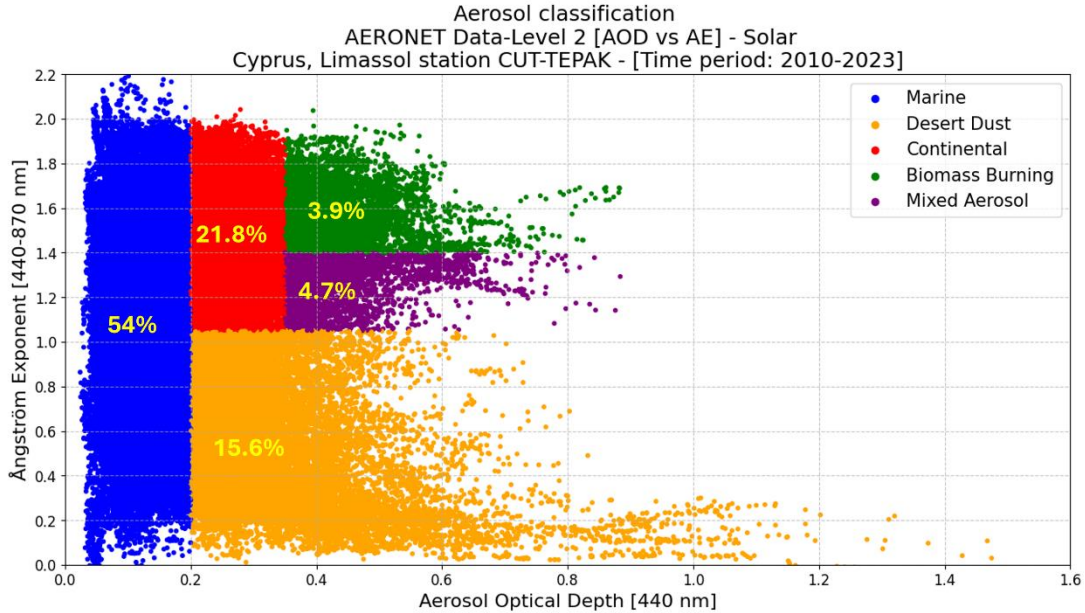


Figure 2. Scatterplot of AOD (440 nm) vs. AE (440-870 nm) distinguishing between five aerosol types for Limassol site, for period 2010 – 2023 with the percentages of each aerosol type using the classification method proposed by Toledano et al. (2007) [1].

Table 4. Aerosol type counts and percentages [%] per season for period [2010-2023].

Aerosol type	Counts per aerosol type [2010-2023]	Aerosol type percentages [%] Spring (M.A.M.) [2010-2023]	Aerosol type percentages [%] Summer (J.J.A.) [2010-2023]	Aerosol type percentages [%] Fall (S.O.N.) [2010-2023]	Aerosol type percentages [%] Winter (D.J.F.) [2010-2023]
Desert dust	23,870	29.3	8.4	13	9.5
Marine	82,638	56.5	41.2	58.9	78.1
Continental	33,361	11.7	33.1	21.9	12.4
Biomass burning	5,976	0.7	7.9	3.3	0.9
Mixed aerosol	7,203	1.8	9.4	3	1.1

The total measurements of AOD-AE optical properties of particles for the CUT-TEPAK station (34.7°N, 33°E) in Limassol, for the period 2010-2023, retrieved from the sun-photometer were 153,048. Aerosols represented in the marine category were the highest percentage of 54% and biomass burning category had the lowest percentage of 3.9%. The Table



4 demonstrates the counts per aerosol type and the seasonally dominant aerosol categories for Limassol area were desert dust (29.3%) in spring, continental (33.1%) and biomass burning (7.9%) particles in summer and marine dominance (58.9%, 78.1%) in fall and winter respectively.

### 3.2 Study of marine aerosol classification area with Particle Depolarization ratio

Aerosol characterization of particulate matter is conducted in the range of  $AOD \leq 0.2$  and  $AE \leq 1$  with the Particle Depolarization ratio at 532 nm. Therefore, the AOD (440 nm) vs AE (440 - 870 nm) diagram provides a qualitative representation of the quantity and size of the particles. The PDR 532 nm represents the sphericity of the aerosols observed in the selected range with the values shown in the graph in color, where blue is the minimum value and red the maximum of PDR (Figure 3).

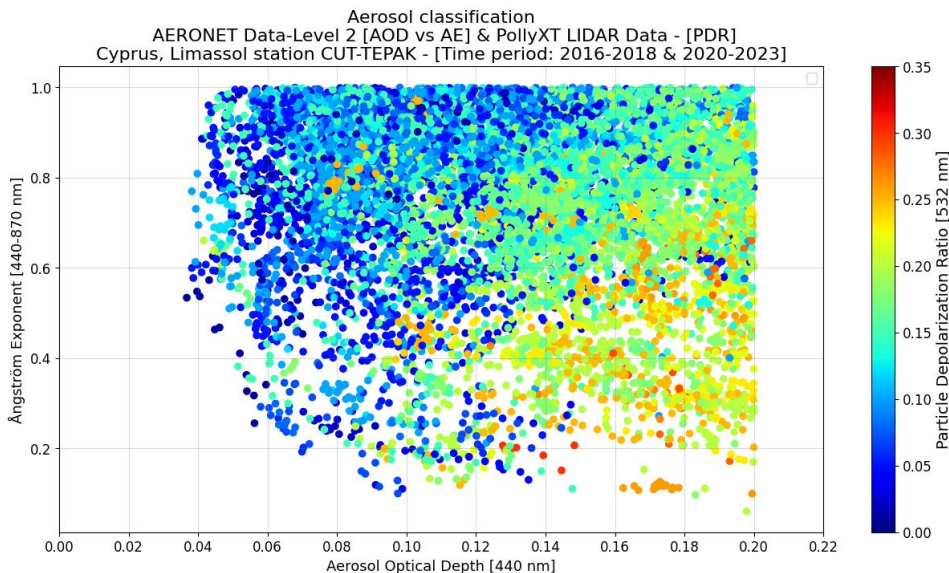


Figure 3. Scatterplot of AOD (440 nm) vs. AE (440-870 nm) in range  $AOD \leq 0.2$ ,  $AE \leq 1$ , for the period 2016-2018 & 2020-2023. The color of each measurement indicates the value of PDR at 532 nm.

Table 5. Counts and percentages [%] of Particle Depolarization ratio.

Particle Depolarization ratio (PDR)	Counts PDR	Percentage of PDR [%]
$\leq 0.05$	1,841	17.47
$> 0.05 \ \& \ \leq 0.1$	2,255	21.39
$> 0.1 \ \& \ \leq 0.15$	2,767	26.25
$> 0.15 \ \& \ \leq 0.2$	2,697	25.59
$> 0.2 \ \& \ \leq 0.25$	900	8.54

According to the study conducted for the Limassol region for six aerosol types by (PhD Argyro Nisantzi, 2015) [50], aerosols were characterized using particle depolarization ratio thresholds at 532 nm. Pure marine particles with PDR values below 0.05 accounting for 17,5% of the measurements. The existence of non-marine particles was observed in the range of  $AOD \leq 0.2$  and  $AE \leq 1$  due to the relatively high particle depolarization ratio values, with 60% percent of the measurements having PDR values above 0.1. The diversity in PDR values highlights the varied aerosol types in the marine aerosol area. Additionally, desert dust particles constituted 9% of the measurements, suggests that particles other than marine may be in the range of  $AOD \leq 0.2$  and  $AE \leq 1$ .

### 3.3 Aerosol classification based on observations of dominating aerosols in Limassol.

This new aerosol typing scheme is based on spectrally resolved long-period LIDAR and sun-photometer observations of the aerosol optical properties: the Aerosol Optical Depth (AOD) and the Ångström Exponent (AE) at Limassol. Therefore, the AOD 440 nm vs AE 440-870 nm diagram describes the quantity and size of particles qualitatively in the aerosols observed at CUT-TEPAK site in Limassol region for the period 2016-2018 & 2020-2023. In the range of  $AOD \leq 0.2$  and  $AE \leq 1$  the aerosol characterization of particulate matter with the PDR at 532 nm is also presented (Figure 4).

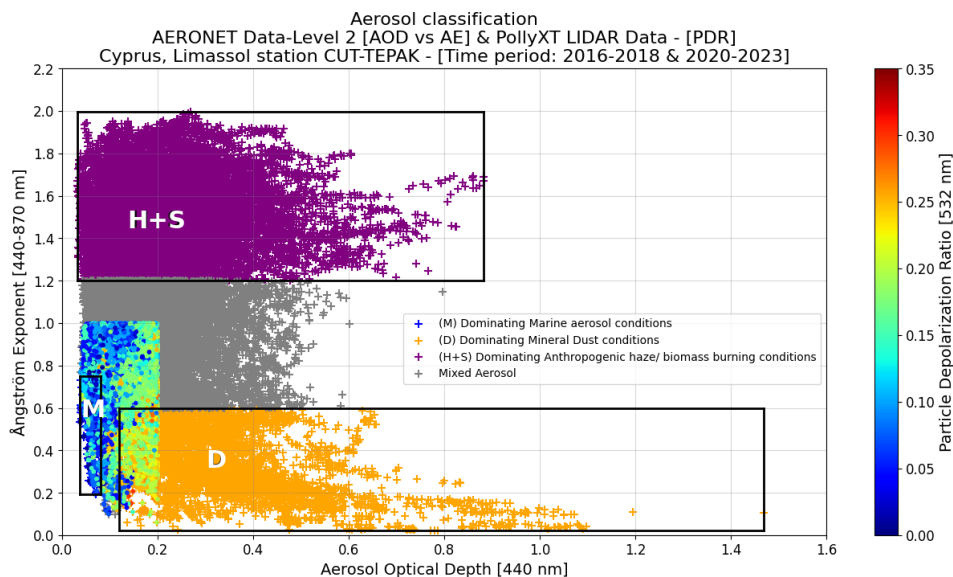


Figure 4. Scatterplot of AOD (440 nm) vs. AE (440-870 nm) distinguishing between four aerosol types using a new aerosol typing scheme for Limassol site, for period 2016-2018 & 2020-2023. Crosses indicate the different aerosol types, dominating conditions of mineral dust (orange), anthropogenic haze/ biomass burning particles (purple), marine aerosol (blue) and mixed aerosol (grey). Different color circles indicate the different PDR values of each measurement.

Table 6. Aerosol type counts and percentages [%] per season for period [2016-2018 & 2020-2023].

Aerosol type	Counts per Aerosol type. [2016-2018 & 2020-2023]	Aerosol type percentages [%] Spring (M.A.M.) [2016-2018 & 2020-2023]	Aerosol type percentages [%] Summer (J.J.A.) [2016-2018 & 2020-2023]	Aerosol type percentages [%] Fall (S.O.N.) [2016-2018 & 2020-2023]	Aerosol type percentages [%] Winter (D.J.F.) [2016-2018 & 2020-2023]
Dominating marine aerosol	561	1.08	0.05	0.44	3.20
Dominating mineral dust	6,512	27.28	1.98	5.08	7.64
Dominating anthropogenic haze/biomass burning	28,763	26.04	74.64	52.89	53.70
Mixed aerosol	20,807	45.61	23.33	41.59	35.47

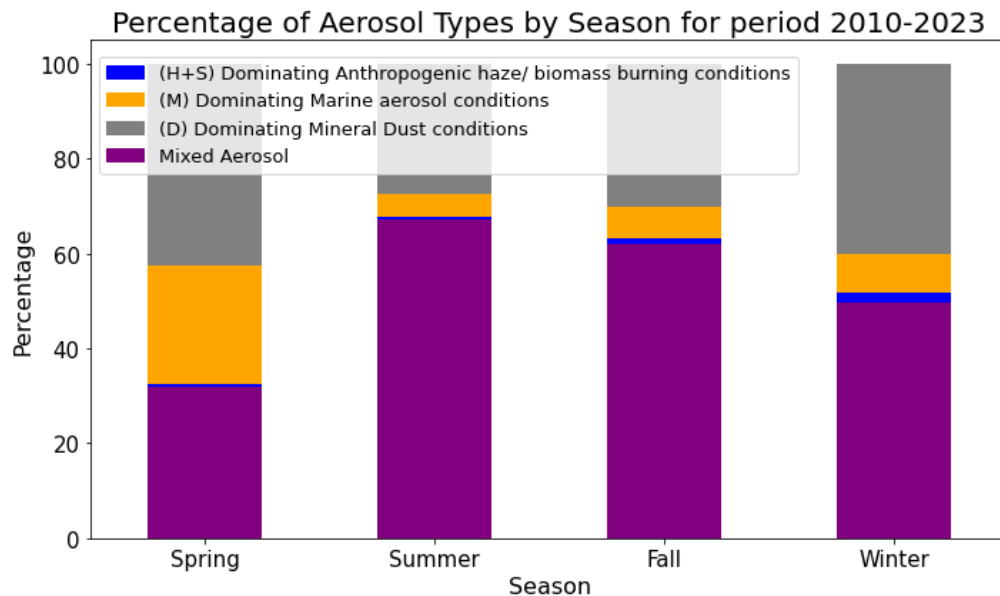


Figure 5. Stacked bar chart showing the seasonal percentages of four aerosol types based on the new aerosol typing scheme for Limassol site, for period 2016-2018 & 2020-2023. Seasons are categorized as spring [M.A.M.], summer [J.J.A.], fall [S.O.N.] and winter [D.J.F.]. Each color indicates the different aerosol types, dominating mineral dust conditions (orange), dominating anthropogenic haze/ biomass burning conditions (purple), dominating marine aerosol conditions (blue), mixed aerosol (grey).

The total measurements of AOD, AE optical properties of particles for the CUT-TEPAK station (34.7°N, 33°E) in Limassol, for the period 2016-2018 & 2020-2023, retrieved from the sun-photometer were 56,643. Aerosols represented in the dominating anthropogenic haze / biomass burning conditions were the highest percentage of 50.78% and dominating marine aerosol conditions category had the lowest percentage of almost 1%. The Table 6 and Figure 5 demonstrates that the seasonally dominant aerosol categories for Limassol area were mixed aerosol (45.61%) and dominating mineral dust conditions (27.28%) in spring, dominating anthropogenic haze / biomass burning conditions (74.64%) in summer and mixed aerosol (41.59%, 35.47%) and dominating anthropogenic haze / biomass burning conditions (52.89%, 53.7%) in fall and winter respectively. During the summer months, especially in August, the atmosphere over Limassol showed a remarkable predominance of anthropogenic haze and biomass burning. A significant presence of mineral dust was observed during April. In contrast, marine particulate matter was present at relatively lower concentrations compared to other pollutants in the atmosphere.

#### 4. CONCLUSIONS

This paper aimed to analyze Limassol's atmospheric composition using remote sensing techniques. A classification method proposed by Toledano et al. (2007) [1] implemented for 14 years (2010-2023) observations of optical properties of aerosol from AERONET products for Limassol (34.7°N, 33°E). The findings revealed that the marine aerosols category was the highest percentage of 54% and biomass burning category had the lowest percentage of 3.9%. Seasonal variations pointed to the dominance of desert dust (29.3%) in spring, continental (33.1%) and biomass burning (7.9%) particles in summer and marine dominance (58.9%, 78.1%) in fall and winter respectively. Further investigation incorporating the particle depolarization ratio (PDR) from the LIDAR vertical profiles at 532 nm using the Klett method, conducted in the range of  $AOD \leq 0.2$  and  $AE \leq 1$  (marine area) for the period 2016-2018 & 2020-2023 revealed nuances. Pure marine particles with PDR values below 0.05 accounting for 17.5% of the measurements. The existence of non-marine particles was observed in the range of  $AOD \leq 0.2$  and  $AE \leq 1$  due to the relatively high PDR values, with 60% of the measurements having values above 0.1 indicating the presence of non-marine particles. Additionally, desert dust particles constituted 9% of the measurements, suggests that particles other than marine may be in the range of  $AOD \leq 0.2$



and  $AE \leq 1$ . Therefore, the classification proposed by Toledano et al. (2007) [1] is not applicable for the Limassol area. The new aerosol typing scheme, based on spectrally resolved extended-term LIDAR and sun-photometer observations at Limassol, portrayed dominating anthropogenic haze / biomass burning conditions were the highest percentage of 50.78% and dominating marine aerosol conditions category had the lowest percentage of almost 1%. Seasonally, in Limassol area mixed aerosol (45.61%) and dominating mineral dust conditions (27.28%) were dominant in spring, dominating anthropogenic haze / biomass burning conditions (74.64%) in summer and mixed aerosol (41.59%, 35.47%) and dominating anthropogenic haze / biomass burning conditions (52.89%, 53.7%) in fall and winter respectively. During the summer months, especially in August, the atmosphere over Limassol showed a remarkable predominance of anthropogenic haze and biomass burning. A significant presence of mineral dust was observed during April. In contrast, marine particulate matter was present at relatively lower concentrations compared to other pollutants in the atmosphere. This integrating approach of aerosol type classification provides insight into the complex aerosol dynamics of Limassol region, contributing knowledge for both atmospheric science and environmental monitoring.

### ACKNOWLEDGEMENTS

The authors acknowledge the ‘EXCELSIOR’: ERATOSTHENES: EXcellence Research Centre for Earth Surveillance and Space-Based Monitoring of the Environment H2020 Widespread Teaming project ([www.excelsior2020.eu](http://www.excelsior2020.eu)). The ‘EXCELSIOR’ project has received funding from the European Union’s Horizon 2020 research and innovation programme under Grant Agreement No 857510, from the Government of the Republic of Cyprus through the Directorate General for the European Programmes, Coordination and Development and the Cyprus University of Technology.

### REFERENCES

- [1] Toledano, C., V. E. Cachorro, A. Berjon, A. M. de Frutos, M. Sorribas, B. A. de la Morena, and P. Goloub. 2007. “Aerosol Optical Depth and Ångström Exponent Climatology at El Arenosillo AERONET Site (Huelva, Spain).” *Quarterly Journal of the Royal Meteorological Society* 133 (624 PART A): 795–807. <https://doi:10.1002/qj.54>.
- [2] You, Wei, Zengliang Zang, Lifeng Zhang, Mei Zhang, Xiaobin Pan, and Yi Li. 2016. “A Nonlinear Model for Estimating Ground-Level PM10 Concentration in Xi’an Using MODIS Aerosol Optical Depth Retrieval.” *Atmospheric Research* 168 (February). Elsevier Ltd: 169–79. <https://doi.org/10.1016/j.atmosres.2015.09.008>
- [3] Kloog, Itai, Meytar Sorek-Hamer, Alexei Lyapustin, Brent Coull, Yujie Wang, Allan C. Just, Joel Schwartz, and David M. Broday. 2015. “Estimating Daily PM2.5 and PM10 across the Complex Geo-Climatic Region of Israel Using MAIAC Satellite-Based AOD Data.” *Atmospheric Environment* 122 (December). Elsevier Ltd: 409–16. <https://doi.org/10.1016/j.atmosenv.2015.10.004>
- [4] Horvath, H., L. Alados Arboledas, F. J. Olmo, O. Jovanović, M. Gangl, W. Kaller, C. Sánchez, H. Sauerzopf, and S. Seidl. 2002. “Optical Characteristics of the Aerosol in Spain and Austria and Its Effect on Radiative Forcing.” *Journal of Geophysical Research Atmospheres* 107 (19). Blackwell Publishing Ltd: AAC 9-1-AAC 9-18. <https://doi.org/10.1029/2001JD001472>
- [5] Meloni, Daniela, A. di Sarra, G. Pace, and F. Monteleone. 2006. “Aerosol Optical Properties at Lampedusa (Central Mediterranean). 2. Determination of Single Scattering Albedo at Two Wavelengths for Different Aerosol Types.” *Atmospheric Chemistry and Physics* 6 (3). European Geosciences Union: 715–27. <https://doi.org/10.5194/acp-6-715-2006>

- [6] Balis, D. S., V. Amiridis, C. Zerefos, E. Gerasopoulos, M. Andreae, P. Zanis, A. Kazantzidis, S. Kazadzis, and A. Papayannis. 2003. "Raman LIDAR and Sunphotometric Measurements of Aerosol Optical Properties over Thessaloniki, Greece during a Biomass Burning Episode." *Atmospheric Environment* 37 (32). Elsevier Ltd: 4529–38. [https://doi.org/10.1016/S1352-2310\(03\)00581-8](https://doi.org/10.1016/S1352-2310(03)00581-8)
- [7] Mamouri, R. E., A. Ansmann, A. Nisantzi, P. Kokkalis, A. Schwarz, and D. Hadjimitsis. 2013. "Low Arabian Dust Extinction-to-Backscatter Ratio." *Geophysical Research Letters* 40 (17). Blackwell Publishing Ltd: 4762–66. <https://doi.org/10.1002/grl.50898>
- [8] Mamouri, R.-E., Ansmann, A., Nisantzi, A., Solomos, S., Kallos, G., and Hadjimitsis, D. G.: Extreme dust storm over the eastern Mediterranean in September 2015: satellite, lidar, and surface observations in the Cyprus region, *Atmos. Chem. Phys.*, 16, 13711– 13724, , 2016, <https://doi.org/10.5194/acp-16-13711-2016>
- [9] Nisantzi, A., R. E. Mamouri, A. Ansmann, and D. Hadjimitsis. 2014. "Injection of Mineral Dust into the Free Troposphere during Fire Events Observed with Polarization LIDAR at Limassol, Cyprus." *Atmospheric Chemistry and Physics* 14 (22). Copernicus GmbH: 12155–65. <https://doi.org/10.5194/acp-14-12155-2014>
- [10] Nisantzi, A., R. E. Mamouri, A. Ansmann, G. L. Schuster, and D. G. Hadjimitsis. 2015. "Middle East versus Saharan Dust Extinction-to-Backscatter Ratios." *Atmospheric Chemistry and Physics* 15 (12). Copernicus GmbH: 7071–84. <https://doi.org/10.5194/acp-15-7071-2015>
- [11] Groß, S., Freudenthaler, V., Haarig, M., Ansmann, A., Toledano, C., Mateos, D., Seibert, P., Mamouri, R.-E., Nisantzi, A., Gasteiger, J., Dollner, M., Tipka, A., Schöberl, M., Teri, M., and Weinzierl, B. 2024. Characterization of aerosol over the Eastern Mediterranean by polarization sensitive Raman lidar measurements during A-LIFE – aerosol type classification and type separation, *EGU sphere* [preprint], <https://doi.org/10.5194/egusphere-2024-140>
- [12] Teri, M., Gasteiger, J., Heimerl, K., Dollner, M., Schöberl, M., Seibert, P., Tipka, A., Müller, T., Aryasree, S., Kandler, K., and Weinzierl, B. 2024. Pollution affects Arabian and Saharan dust optical properties in the Eastern Mediterranean, *EGU sphere* [preprint], <https://doi.org/10.5194/egusphere-2024-701>
- [13] Cappa, Christopher D., Katheryn R. Kolesar, Xiaolu Zhang, Dean B. Atkinson, Mikhail S. Pekour, Rahul A. Zaveri, Alla Zelenyuk, and Qi Zhang. 2016. "Understanding the Optical Properties of Ambient Sub-and Supermicron Particulate Matter: Results from the CARES 2010 Field Study in Northern California." *Atmospheric Chemistry and Physics* 16 (10). Copernicus GmbH: 6511–35. <https://doi.org/10.5194/acp-16-6511-2016>
- [14] Romano, Salvatore, Maria Rita Perrone, Giulia Pavese, Francesco Esposito, and Mariarosaria Calvello. 2019. "Optical Properties of PM<sub>2.5</sub> Particles: Results from a Monitoring Campaign in Southeastern Italy." *Atmospheric Environment* 203 (April). Elsevier Ltd: 35–47. <https://doi.org/10.1016/j.atmosenv.2019.01.037>
- [15] Rupakheti, Dipesh, Shichang Kang, Maheswar Rupakheti, Zhiyuan Cong, Arnico K. Panday, and Brent N. Holben. 2019. "Identification of Absorbing Aerosol Types at a Site in the Northern Edge of Indo-Gangetic Plain and a Polluted Valley in the Foothills of the Central Himalayas." *Atmospheric Research* 223 (July). Elsevier Ltd: 15–23. <https://doi.org/10.1016/j.atmosres.2019.03.003>
- [16] Ali, Md Arfan, Janet E. Nichol, Muhammad Bilal, Zhongfeng Qiu, Usman Mazhar, Md Wahiduzzaman, Mansour Almazroui, and M. Nazrul Islam. 2020. "Classification of Aerosols over Saudi Arabia from 2004–2016." *Atmospheric Environment* 241 (November). Elsevier Ltd. <https://doi.org/10.1016/j.atmosenv.2020.117785>
- [17] Bilal, Muhammad, Alaa Mhawish, Janet E. Nichol, Zhongfeng Qiu, Majid Nazeer, Md Arfan Ali, Gerrit de Leeuw, et al. 2021. "Air Pollution Scenario over Pakistan: Characterization and Ranking of Extremely Polluted Cities Using

Long-Term Concentrations of Aerosols and Trace Gases.” Remote Sensing of Environment 264 (October). Elsevier Inc. <https://doi.org/10.1016/j.rse.2021.112617>

- [18] Russell, P. B., R. W. Bergstrom, Y. Shinozuka, A. D. Clarke, P. F. Decarlo, J. L. Jimenez, J. M. Livingston, J. Redemann, O. Dubovik, and A. Strawa. 2010. “Absorption Ångström Exponent in AERONET and Related Data as an Indicator of Aerosol Composition.” Atmospheric Chemistry and Physics 10 (3). Copernicus GmbH: 1155–69. <https://doi.org/10.5194/acp-10-1155-2010>
- [19] Giles, David M., Brent N. Holben, Sachchida N. Tripathi, Thomas F. Eck, W. Wayne Newcomb, Ilya Slutsker, Russell R. Dickerson, et al. 2011. “Aerosol Properties over the Indo-Gangetic Plain: A Mesoscale Perspective from the TIGERZ Experiment.” Journal of Geophysical Research Atmospheres 116 (18). Blackwell Publishing Ltd. <https://doi.org/10.1029/2011JD015809>
- [20] Giles, D. M., B. N. Holben, T. F. Eck, A. Sinyuk, A. Smirnov, I. Slutsker, R. R. Dickerson, A. M. Thompson, and J. S. Schafer. 2012. “An Analysis of AERONET Aerosol Absorption Properties and Classifications Representative of Aerosol Source Regions.” Journal of Geophysical Research Atmospheres 117 (17). Blackwell Publishing Ltd. <https://doi.org/10.1029/2012JD018127>
- [21] Toledano, C., M. Wiegner, S. Groß, V. Freudenthaler, J. Gasteiger, D. Müller, T. Müller, et al. 2011. “Optical Properties of Aerosol Mixtures Derived from Sun-Sky Radiometry during SAMUM-2.” Tellus, Series B: Chemical and Physical Meteorology 63 (4): 635–48. <https://doi.org/10.1111/j.1600-0889.2011.00573.x>
- [22] Cazorla, A., R. Bahadur, K. J. Suski, J. F. Cahill, D. Chand, B. Schmid, V. Ramanathan, and K. A. Prather. 2013. “Relating Aerosol Absorption Due to Soot, Organic Carbon, and Dust to Emission Sources Determined from in-Situ Chemical Measurements.” Atmospheric Chemistry and Physics 13 (18): 9337–50. <https://doi.org/10.5194/acp-13-9337-2013>
- [23] Artemis Voudouri, K., Siomos, N., Michailidis, K., Papagiannopoulos, N., Mona, L., Cornacchia, C., ... Balis, D. (2019). Comparison of two automated aerosol typing methods and their application to an EARLINET station. Atmospheric Chemistry and Physics, 19(16), 10961–10980. <https://doi.org/10.5194/acp-19-10961-2019>
- [24] Kaskaoutis, Dimitris G., Georgios Grivas, Christina Theodosi, Maria Tsagkaraki, Despina Paraskevopoulou, Iasonas Stavroulas, Eleni Liakakou, et al. 2020. “Carbonaceous Aerosols in Contrasting Atmospheric Environments in Greek Cities: Evaluation of the EC-Tracer Methods for Secondary Organic Carbon Estimation.” Atmosphere 11 (2). MDPI AG. <https://doi.org/10.3390/atmos11020161>
- [25] Kaskaoutis, D. G., H. D. Kambezidis, N. Hatzianastassiou, P. G. Kosmopoulos, and K. V. S. Badarinath. 2007. “Aerosol Climatology: On the Discrimination of Aerosol Types over Four AERONET Sites.” Atmospheric Chemistry and Physics Discussions 7 (3). Copernicus GmbH: 6357–6411. <https://doi.org/10.5194/acpd-7-6357-2007>
- [26] Dubovik, Oleg, Brent Holben, Thomas F. Eck, Alexander Smirnov, Yoram J. Kaufman, Michael D. King, Didier Tanré, and Ilya Slutsker. 2002. “Variability of Absorption and Optical Properties of Key Aerosol Types Observed in Worldwide Locations.” Journal of the Atmospheric Sciences 59 (3): 590–608. [https://doi.org/10.1175/1520-0469\(2002\)059<0590:VOAAOP>2.0.CO;2](https://doi.org/10.1175/1520-0469(2002)059<0590:VOAAOP>2.0.CO;2)
- [27] Gobbi, G. P., Y. J. Kaufman, I. Koren, and T. F. Eck. 2007. “Classification of Aerosol Properties Derived from AERONET Direct Sun Data.” Atmospheric Chemistry and Physics 7 (2). European Geosciences Union: 453–58. <https://doi.org/10.5194/acp-7-453-2007>

- [1] Tesche, M., A. Ansmann, D. Müller, D. Althausen, R. Engelmann, V. Freudenthaler, and S. Groß. 2009. “Vertically Resolved Separation of Dust and Smoke over Cape Verde Using Multiwavelength Raman and Polarization LIDARs during Saharan Mineral Dust Experiment 2008.” *Journal of Geophysical Research Atmospheres* 114 (13). Blackwell Publishing Ltd. <https://doi.org/10.1029/2009JD011862>
- [28] Tesche, Matthias, Detlef Müller, Silke Gross, Albert Ansmann, Dietrich Althausen, Volker Freudenthaler, Bernadett Weinzierl, Andreas Veira, and Andreas Petzold. 2011. “Optical and Microphysical Properties of Smoke over Cape Verde Inferred from Multiwavelength LIDAR Measurements.” *Tellus, Series B: Chemical and Physical Meteorology* 63 (4): 677–94. <https://doi.org/10.1111/j.1600-0889.2011.00549.x>
- [29] Ansmann, A., M. Tesche, P. Seifert, S. Groß, V. Freudenthaler, A. Apituley, K. M. Wilson, et al. 2011. “Ash and Fine-Mode Particle Mass Profiles from EARLINET-AERONET Observations over Central Europe after the Eruptions of the Eyjafjallajökull Volcano in 2010.” *Journal of Geophysical Research Atmospheres* 116 (12). Blackwell Publishing Ltd. <https://doi.org/10.1029/2010JD015567>
- [30] Ansmann, A., Seifert, P., Tesche, M., & Wandinger, U. (2012). Profiling of fine and coarse particle mass: Case studies of Saharan dust and Eyjafjallajökull/Grimsvötn volcanic plumes. *Atmospheric Chemistry and Physics*, 12(20), 9399–9415. <https://doi.org/10.5194/acp-12-9399-2012>
- [31] Mamouri, R. E., and A. Ansmann. 2014. “Fine and Coarse Dust Separation with Polarization LIDAR.” *Atmospheric Measurement Techniques* 7 (11). Copernicus Publications: 3717–35. <https://doi.org/10.5194/amt-7-3717-2014>
- [32] Ångström, Anders. 1961. “Techniques of Determining the Turbidity of the Atmosphere.” *Tellus* 13 (2). Stockholm University Press: 214–23. <https://doi.org/10.3402/tellusa.v13i2.9493>
- [33] Westphal, D. L., and O. B. Toon. 1991. “Simulations of Microphysical, Radiative, and Dynamical Processes in a Continental-Scale Forest Fire Smoke Plume.” *Journal of Geophysical Research* 96 (D12). <https://doi.org/10.1029/91JD01956>
- [34] Eck, T. F., B. N. Holben, J. S. Reid, O. Dubovik, A. Smirnov, N. T. O’Neill, I. Slutsker, and S. Kinne. 1999. “Wavelength Dependence of the Optical Depth of Biomass Burning, Urban, and Desert Dust Aerosols.” *Journal of Geophysical Research Atmospheres* 104 (D24). Blackwell Publishing Ltd: 31333–49. <https://doi.org/10.1029/1999JD900923>
- [35] Giannakaki, E., D. S. Balis, V. Amiridis, and C. Zerefos. 2010. “Optical Properties of Different Aerosol Types: Seven Years of Combined Raman-Elastic Backscatter LIDAR Measurements in Thessaloniki, Greece.” *Atmospheric Measurement Techniques* 3 (3): 569–78. <https://doi.org/10.5194/amt-3-569-2010>
- [36] Sassen, K. 1991. “The Polarization LIDAR Technique for Cloud Research: A Review and Current Assessment.” *Bulletin - American Meteorological Society* 72 (12): 1848–66. [https://doi.org/10.1175/1520-0477\(1991\)072<1848:TPLTFC>2.0.CO;2](https://doi.org/10.1175/1520-0477(1991)072<1848:TPLTFC>2.0.CO;2)
- [37] Ansmann, Albert, Ina Mattis, Detlef Müller, Ulla Wandinger, Marcus Radlach, Dietrich Althausen, and Richard Damoah. 2005. “Ice Formation in Saharan Dust over Central Europe Observed with Temperature/Humidity/Aerosol Raman LIDAR.” *Journal of Geophysical Research D: Atmospheres* 110 (18): 1–12. <https://doi.org/10.1029/2004JD005000>
- [38] Murayama, Toshiyuki, Hajime Okamoto, Naoki Kaneyasu, Hiroki Kamataki, and Kazuhiko Miura. 1999. “Application of LIDAR Depolarization Measurement in the Atmospheric Boundary Layer: Effects of Dust and Sea-Salt Particles.” *Journal of Geophysical Research Atmospheres* 104 (D24). Blackwell Publishing Ltd: 31781–92. <https://doi.org/10.1029/1999JD900503>

- [39] Sakai, Tetsu, Tomohiro Nagai, Yuji Zaizen, and Yuzo Mano. 2010. “Backscattering Linear Depolarization Ratio Measurements of Mineral, Sea-Salt, and Ammonium Sulfate Particles Simulated in a Laboratory Chamber.” *Applied Optics* 49 (23). OSA - The Optical Society: 4441–49. DOI:[10.1364/AO.49.004441](https://doi.org/10.1364/AO.49.004441)
- [40] Groß, Silke, Matthias Tesche, Volker Freudenthaler, Carlos Toledano, Matthias Wiegner, Albert Ansmann, Dietrich Althausen, and Meinhard Seefeldner. 2011. “Characterization of Saharan Dust, Marine Aerosols and Mixtures of Biomass-Burning Aerosols and Dust by Means of Multi-Wavelength Depolarization and Raman Lidar Measurements during SAMUM 2.” *Tellus, Series B: Chemical and Physical Meteorology* 63 (4): 706–24. <https://doi.org/10.1111/j.1600-0889.2011.00556.x>
- [41] Holben, Brent N., T. F. Eck, I. Slutsker, D. Tanré, J. P. Buis, A. Setzer, E. Vermote, et al. 1998. “AERONET - A Federated Instrument Network and Data Archive for Aerosol Characterization.” *Remote Sensing of Environment* 66 (1). Elsevier Science Inc: 1–16. [https://doi.org/10.1016/S0034-4257\(98\)00031-5](https://doi.org/10.1016/S0034-4257(98)00031-5)
- [42] AERONET: Aerosol Robotic Network aerosol data base, National Aeronautics and Space Administration (NASA) [data set], <http://aeronet.gsfc.nasa.gov/>, last access: 06 March 2024.
- [43] G., Hadjimitsis, Rodanthi-Elisavet Mamouri, Argyro Nisantzi, Natalia Kouremerti, Adrianos Retalis, Dimitris Paronis, Filippos Tymvios, et al. 2013. “Air Pollution from Space.” In *Remote Sensing of Environment - Integrated Approaches*. InTech. <https://doi.org/10.5772/39310>
- [44] Engelmann, Ronny, Thomas Kanitz, Holger Baars, Birgit Heese, Dietrich Althausen, Annett Skupin, Ulla Wandinger, et al. 2016. “The Automated Multiwavelength Raman Polarization and Water-Vapor Lidar PollyXT: The neXT Generation.” *Atmospheric Measurement Techniques* 9 (4). Copernicus GmbH: 1767–84. <https://doi.org/10.5194/amt-9-1767-2016>
- [45] ACTRIS: Aerosols, Clouds and Trace gases Research InfraStructure home page, <https://www.actris.eu/>, last access: 06 March 2024.
- [46] Klett, J. D. 1981. “Stable analytic inversion solution for processing LIDAR returns”, *Appl. Optics*, 20, 211–220. DOI: [10.1364/AO.20.000211](https://doi.org/10.1364/AO.20.000211)
- [47] Ozdemir, Esra, Gizem Tuna Tuygun, and Tolga Elbir. 2020. “Application of Aerosol Classification Methods Based on AERONET Version 3 Product over Eastern Mediterranean and Black Sea.” *Atmospheric Pollution Research* 11 (12). Elsevier B.V.: 2226–43. <https://doi.org/10.1016/j.apr.2020.06.008>
- [48] Smirnov, A., B. N. Holben, O. Dubovik, R. Frouin, T. F. Eck, and I. Slutsker. 2003. “Maritime Component in Aerosol Optical Models Derived from Aerosol Robotic Network Data.” *Journal of Geophysical Research: Atmospheres* 108 (1). Blackwell Publishing Ltd. <https://doi.org/10.1029/2002JD002701>
- [49] Nisantzi A. 2015 ‘Μελέτη της Ατμόσφαιρας και των οπτικών ιδιοτήτων των αιωρούμενων σωματιδίων με τη συνδυασμένη χρήση τηλεπισκόπησης και τεχνικών LIDAR στην περιοχή της Ανατολικής Μεσογείου’ PhD thesis, Cyprus University of Technology, Cyprus, p91, 193-202, <https://ktisis.cut.ac.cy/handle/20.500.14279/8461>